International Journal of Energetic Materials and Chemical Propulsion, 11 (3): 259–273 (2012)

COMBUSTION OF BIMODAL ALUMINUM PARTICLES AND ICE MIXTURES

Terrence L. Connell, Jr.,[1] Grant A. Risha,[1,*] Richard A. Yetter,[1] Vigor Yang,[2] & Steven F. Son[3]

[1] *Department of Mechanical and Nuclear Engineering, The Pennsylvania State University, University Park, Pennsylvania 16802, USA*

[2] *School of Aerospace Engineering, Georgia Institute of Technology, Atlanta, Georgia 30332, USA*

[3] *School of Mechanical Engineering, Purdue University, West Lafayette, Indiana 47907, USA*

[*] Address all correspondence to Grant A. Risha E-mail: gar108@psu.edu

The combustion of aluminum with ice is studied using various mixtures of nano- and micrometer-sized aluminum particles as a means to generate high-temperature hydrogen at fast rates for propulsion and power applications. Bimodal distributions are of interest in order to vary mixture packing densities and nascent alumina concentrations in the initial reactant mixture. In addition, the burning rate can be tailored by introducing various particle sizes. The effects of the bimodal distributions and equivalence ratio on ignition, combustion rates, and combustion efficiency are investigated in strand experiments at constant pressure and in small lab-scale [1.91 cm (0.75 in.) diameter] static fired-rocket-motor combustion chambers with center-perforated propellant grains. The aluminum particles consisted of nanometer-sized particles with a nominal diameter of 80 nm and micron-sized particles with nominal diameters of 2 and 5 μm. The micron particle addition ranged from 0% to 80% by active mass in the mixture. Burning rates from 1.1 (160 psia) to 14.2 MPa (2060 psia) were determined. From the small scale motor experiments, thrust, C^*, Isp, and C^* and Isp efficiencies are provided. From these results, mechanistic issues of the combustion process are discussed. In particular, overall lean equivalence ratios that produce flame temperatures near the melting point of alumina resulted in considerably lower experimental C^* and Isp efficiencies than equivalence ratios closer to stoichiometric. The substitution of micron aluminum for nanometer aluminum had little effect on the linear burning rates of Al/ice mixtures for low-mass substitutions. However, as the mass addition of micron aluminum increased (e.g., beyond 40% 2-μm aluminum in place of 80-nm aluminum), the burning rates decreased. The effects of bimodal aluminum compositions on motor performance were minor, although the experimental results suggest longer combustion times are necessary for complete combustion.

KEY WORDS: *solid hydrogen storage, hydrogen generation, propulsion, green propellants, combustion rates*

2150–766X/12/$35.00

NOMENCLATURE

I_{tot}	total impulse (N·s)	C^*	characteristic exhaust velocity (m/s)
D_t	nozzle throat diameter (cm)	ϕ or phi	equivalence ratio (—)
r_b	propellant burning rate (cm/s)	$\eta_{Isp,\text{avg}}$ or Isp efficiency	specific impulse efficiency $Isp_{\text{meas}}/Isp_{\text{theor}}$
P	average chamber pressure (MPa)	$\eta_{C^*,\text{avg}}$ or C^* efficiency	characteristic exhaust velocity $C^*_{\text{meas}}/C^*_{\text{theor}}$

1. INTRODUCTION

Mixtures of aluminum and water have been studied for many years because of the high heat release and gas-phase production of molecular hydrogen associated with this reaction (Yetter, 2009). For mixtures with micron-sized particles, reaction rates are slow; flame propagation through unfrozen (liquid water) and frozen (ice) mixtures does not occur. However, Ivanov et al. (1995, 2000) showed that mixtures of nAl, water, and polyacrylamide could propagate a self-sustaining reaction. Risha et al. (2006, 2007, 2008) showed that propagation was possible without a gelling agent or surfactant. Recently, several groups have proposed nAl and water mixtures for space propulsion (Ingenito and Bruno, 2004; Miller and Herr, 2004; Risha et al., 2006). Franson et al. (2007a,b) studied composite motors consisting of Al, H_2O, and H_2O_2. No performance characteristics were reported. Risha et al. (2009, 2013) studied a nAl/ice propellant (named ALICE) and developed a center-perforated composite grain motor in which scaling studies were performed in three different size motors to evaluate performance. This propellant and motor design was recently tested in a small-scale sounding rocket by Pourpoint et al. (2012).

The propellant studied by Risha et al. (2009, 2013) and Connell (2011) consisted of 80-nm aluminum and ice with an overall equivalence ratio of 0.71. Nanometer aluminum particles can have a significantly thick oxide layer covering the particle surface, thus passivating the aluminum and preventing pyrophoric reaction. For the 80-nm aluminum used by Risha et al. (2009, 2013), 74.5% of the aluminum particle mass consisted of active aluminum. The remaining 25.5% mass was inert and consisted of aluminum oxide. From a performance perspective, specific impulse, which may be evaluated from the total impulse delivered by the motor divided by the mass of the propellant, suffers a significant loss as a consequence of the presence of the thick oxide layers on nAl. Because micron particles have a significantly larger fraction of active aluminum content (generally between 95% and 99%), the performance of the aluminum and ice propellants may simply be improved by replacing a portion of the nanometer aluminum with micron

aluminum provided combustion rates remain fast enough to achieve complete combustion in the short available residence times.

Figure 1 illustrates the increase in active content of the aluminum fuel consisting of a bimodal particle distribution as nanometer particles with a nominal diameter of 80 nm are replaced with micron particles. Progressing from a pure nanoparticle fuel to a particle with a 50% nAl and 50% μm Al (by mass) consistency, the active aluminum content increases by ∼13%. Figure 2 shows the manner in which this change in active aluminum

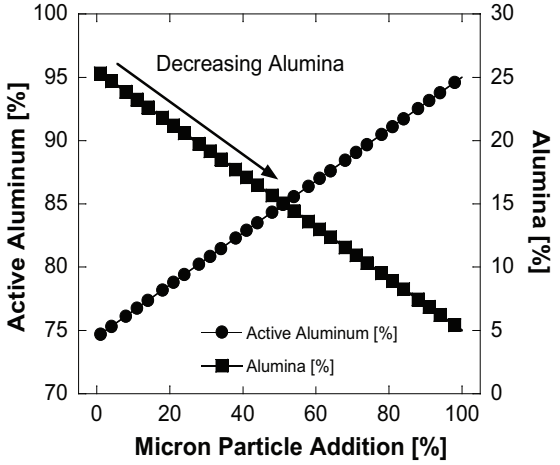

FIG. 1: Active aluminum content versus bimodal aluminum distribution assuming a 95% active aluminum content for the micron aluminum.

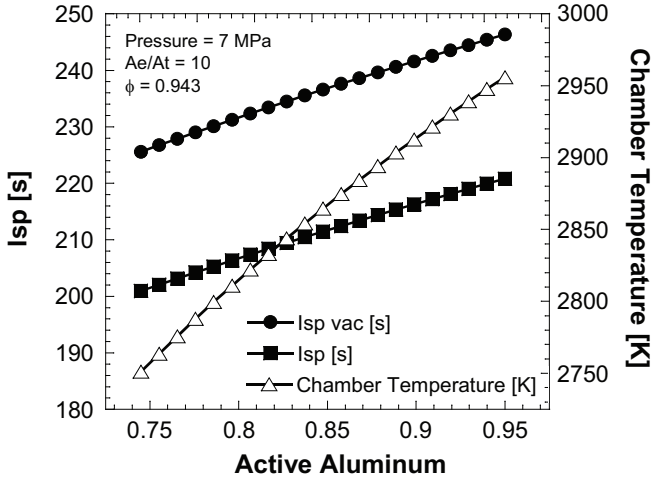

FIG. 2: Theoretical results Isp and chamber temperature as a function of the active aluminum content in for ϕ = 0.943; the calculations were performed with CEA (McBride and Gordon, 1996).

content affects the flame temperature and specific impulse (Isp) of the propellant. The flame temperature increases by ∼110 K and the Isp increases by ∼11 s by replacing 50% of the mass of 80-nm aluminum with micron-sized aluminum.

In the present paper, composite propellants of nAl and ice are studied in which the fuel is a mixture of nanometer and micron aluminum. The addition of micron aluminum to a base fuel consisting only of nanometer aluminum is studied to reduce the initial alumina (inert mass) in the composite propellant and to provide control of the burning rate independent of the mixture ratio. The effects of equivalence ratio are also studied because changes in the particle size distribution also affect the mixture consistency (Risha et al., 2007). Linear burning rate measurements are performed as a function of micron aluminum content in the fuel mixture, equivalence ratio, and pressure. Motor performance studies are performed with a center-perforated grain in a small laboratory-scale 1.91-cm (0.75-in.) diameter motor.

2. EXPERIMENTAL PROCEDURE

The propellant reactants consisted of nanometer and micron aluminum and de-ionized water. The nanoaluminum particles were obtained from Nanotechnologies, Inc., and had a nominal diameter of 80 nm. The micron aluminum particles were obtained from Valimet and had nominal diameters of 2 and 5 μm. Scanning electron microscopy images of the 80-nm and 2-μm aluminum are shown in Fig. 3. Both sizes of particles had spherical shapes. The active aluminum content of the "as received" nanometer aluminum was generally around 77%–79%. However, in the present studies, just as in our previous studies, further passivation of the nanometer aluminum was performed to achieve an active content of ∼74% (Risha et al., 2009, 2013). The aluminum was characterized using simultaneous thermogravimetric analysis and differential scanning calorimetry. The active aluminum content of the aluminum sample was back-calculated from the mass gain assuming all of the active aluminum was converted to alumina and the particles were

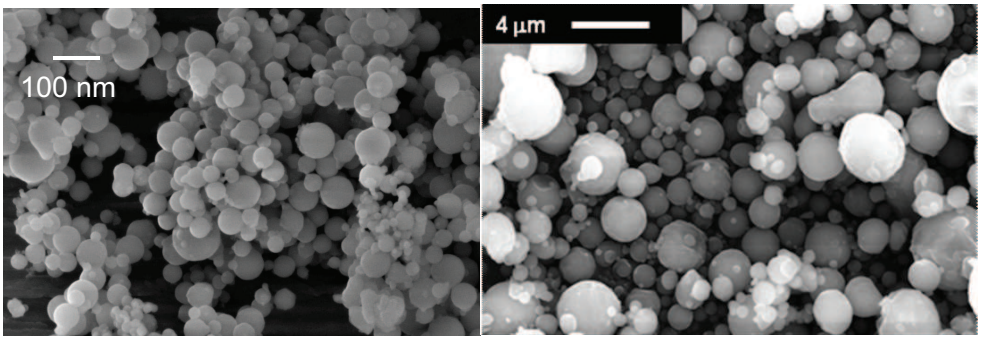

(courtesy of Mr. Ed Roemer) (courtesy of Dr. Justin Sabourin)

FIG. 3: SEMs of 80-nm and 2-μm aluminum particles.

spheres. The additional passivation was performed to minimize any low-temperature oxidation with the liquid water during mixing prior to freezing. Once the mixtures were frozen, no oxidation of the nAl was observed. An active aluminum content of 98.6% was used for both the 2- and 5-μm Al particles.

For all mixtures with combined nanometer- and micron-sized aluminum, a Resodyn LabRAM mixer was used to premix particles. De-ionized water was then added to the bimodal powder mixture and the final mixing was performed by hand. As more micron aluminum was added to the mixture for a given overall stoichiometry, the mixture consistency changed from a claylike to a paste to a slurry mixture. The more fluidic, less viscous, mixture resulted from the significantly lower surface area of the micron versus nanometer aluminum. For an equivalence ratio of 0.71, a micron aluminum content of ∼20% relative to the total active aluminum content could be achieved prior to significant settling of the micron aluminum in the unfrozen mixture. For an equivalence ratio of 0.943, a micron content of ∼80% was achievable prior to significant settling of the micron aluminum. As a consequence, most of the combustion studies considered here were performed with an equivalence ratio of 0.943. After packing the tube molds, either for strand experiments or scale motor experiments, the material was placed in an explosion-proof freezer and stored at –30°C. Phenolic tubes were used for the motor grains while quartz tubes were used for the strand burner experiments. Densities varied with the micron aluminum content of the mixture and are illustrated in Fig. 4. For mixtures with an overall equivalence ratio of 0.943, a decrease in mixture density from about 1.57 to 1.45 g/cm^3 was observed with the substitution of 80% of the aluminum mass with either 2- or 5-μm aluminum.

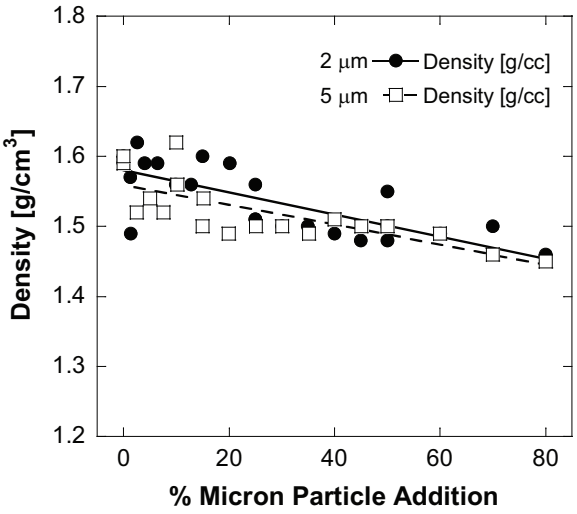

FIG. 4: Mixture density as a function of micron Al substitution of nanometer aluminum in bimodal mixtures with an equivalence ratio of 0.943.

2.1 Propellant Strand Burner

Steady-state, constant-volume strand burner experiments were performed to evaluate the linear burning rates of the bimodal aluminum ice mixtures. The chamber, constructed from 316 stainless steel, was equipped with four optical viewing ports each having a 15.2 $\times$ 2.54 cm field of view and feedthroughs in the base plate allowing both electrical signal and gas pathways into the chamber. The 61-cm-long chamber has an inner diameter of 22 cm and a total free volume of 23 L to minimize the pressure variation caused by the generation of gaseous combustion products during an experiment. One of the optical viewing ports was backlit through an optical diffuser while the opposite viewing port from the diffuser was used for real-time recording of the burning process by a Sony digital video camera. The operating pressure was varied from 1.1 to 14.2 MPa. The initial propellant temperature for the ALICE samples was approximately –30°C. Argon was used as the pressurant gas and a Setra 206 pressure transducer was used to measure the instantaneous chamber pressure. Ignition was achieved by igniting a classical double-base propellant (NOSOL 363) by a resistance wire, thereby igniting the ALICE strand. Burning rates were determined as functions of micron aluminum content, nominal micron particle size, and pressure. For each experiment, the sample was ignited at a specific pressure, and the steady-state linear burning rate was recorded. Distance versus time curves were constructed from the recorded video. Thus, the burning rate for that specific pressure was obtained from the slope of the curves. The aluminum water mixtures were packed in 10 mm O.D.$\times$8 mm I.D. quartz tubes prior to freezing. These samples were tested in the frozen state while in the quartz tubes.

2.2 Solid Propellant Motor

A lab-scale motor with combustion chamber diameter of 1.91 cm (0.75 in.) was used to evaluate the performance of the ALICE propellant. The motor was operated in a center-perforated grain configuration. The grain lengths were 7.62 cm with a 0.635-cm-diameter center port. A post combustion chamber with a length of 7.62 cm and diameter of 1.91 cm was used. The motor chamber was equipped with two Setra pressure transducers to monitor the chamber pressure. The pressure transducers were located at the aft end of the motor and recorded pressure through porting within the post-combustion chamber liner. Two transducers were used for a multitude of reasons, primarily, if one were to become clogged with alumina, the second would hopefully remain unrestricted, and therefore record accurate chamber pressure. Secondly, having two pressure transducers reveals any substantial harmonics within the chamber. Burst discs were installed to prevent any over-pressurization. The graphite nozzle had conical converging and diverging sections with the diverging section employing an expansion ratio of 10 and a divergence half-angle of 15°. The throat diameter for the present motor experiments was 0.409 cm (0.161 in.). Ignition was achieved using a commercially available Estes C6-0 and A10-PT model rocket motors. The igniter motors were initiated with a small squib

that required a 5-V dc input. An OMEGA load cell (220 N) was used to determine the instantaneous thrust of the motor, which was mounted on a thrust sled allowing only one degree of freedom in the axial direction. Data were recorded at 5 kHz using a custom LabVIEW data acquisition program. ALICE grains were cartridge loaded for ease of assembly and reduced testing time. A more detailed description of the motor and experimental setup can be found in Risha et al. (2009, 2013).

3. RESULTS AND DISCUSSION

The results of burning rate are provided first, followed by measurements on the performance of the center-perforated ALICE grain motor. The effect of equivalence ratio using frozen 80-nm aluminum-ice grains has been studied.

3.1 Burning Rate Measurements

Figure 5 shows exemplary trajectory plots of the flame position in the 8-mm I.D. quartz tubes as a function of time for three pressures and a 75% nAl/25% μAl and ice mixture with an equivalence ratio of 0.943. Steady-state flame propagation was observed for all the reported results.

The burning rates for mixtures of 80-nm aluminum with 2-μm aluminum at targeted pressure of 7 MPa (1014.7 psia) are shown in Fig. 6. Burning rates for mixtures of 80-nm and 5-μm aluminum at the same conditions are shown in Fig. 7. For both sizes of micron particles, a slight increase in burning rate is observed with the addition of small amounts

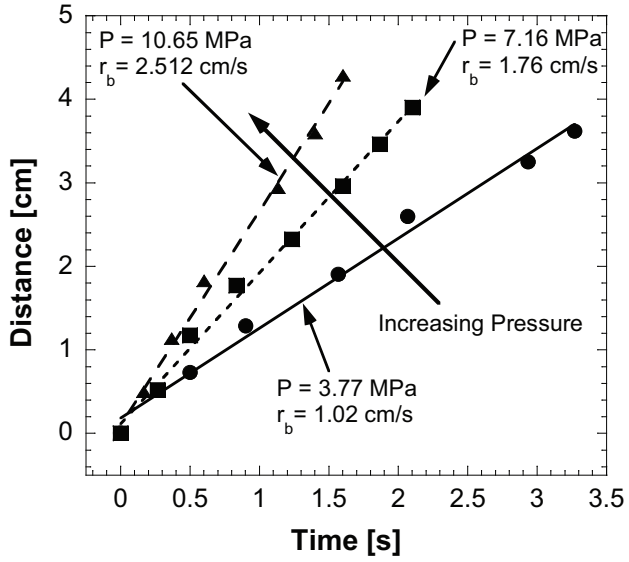

FIG. 5: Trajectory plots of strand burning distance versus time.

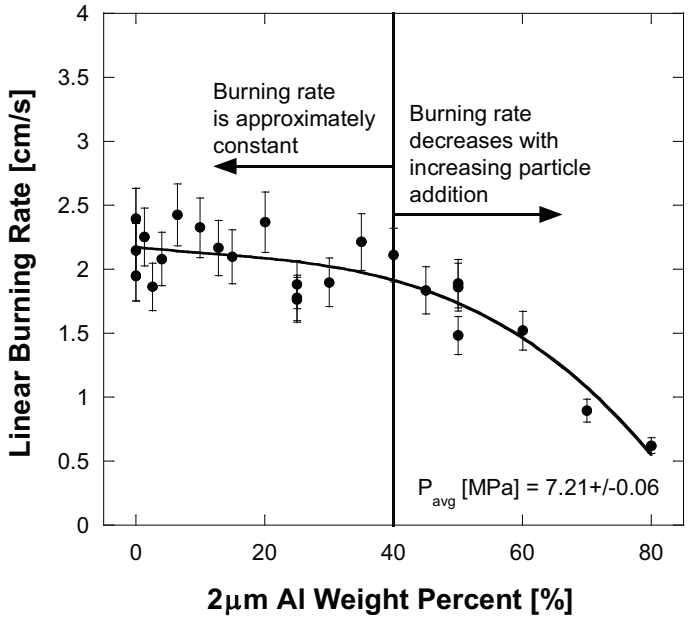

FIG. 6: Linear burning rate as a function of 2-μm aluminum content in the fuel mixture for an equivalence ratio of 0.943 and target pressure of 7 MPa (1014.7 psia).

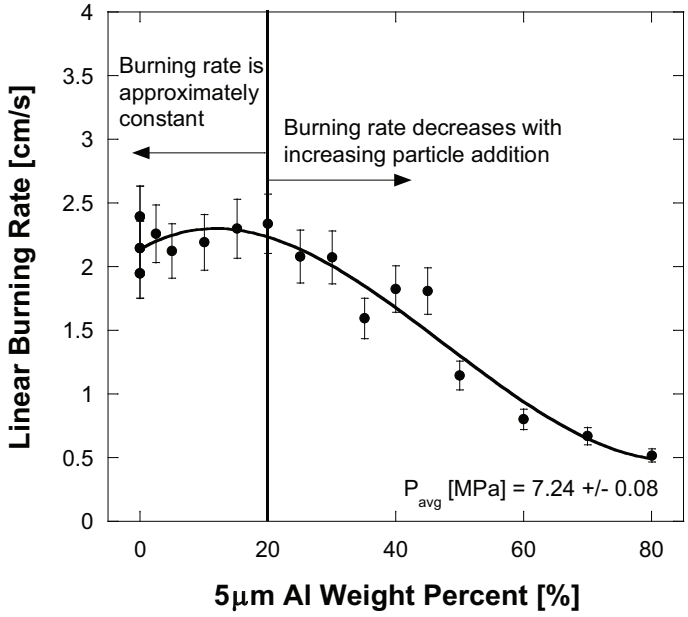

FIG. 7: Linear burning rate as a function of 5-μm aluminum content in the fuel mixture for an equivalence ratio of 0.943 and target pressure of 7 MPa (1014.7 psia).

of micron aluminum. The addition of large amounts of micron aluminum decreases the burning rate. The decrease in burning rate is evident at a lower amount of substituted micron aluminum for the 5-μm aluminum (∼20%) compared to the 2-μm aluminum (∼40%). The slight increase in burning rate likely results from a slightly higher reaction temperature due to lesser inert alumina initially present in the mixture. However, as the amount of micron aluminum increases, the propagation rate becomes more rate limited by the larger particles than any further increase in reaction temperature and the burning rate decreases. The results suggest that in addition to reducing alumina in the initial mixture, bimodal distributions may be used to control burning rates.

Figure 8 shows the burning rate as a function of pressure for mixtures with only 80-nm aluminum and mixtures with substitution of 25% and 50% (based upon the active aluminum mass) of the 80-nm aluminum with 2-μm aluminum. The overall equivalence ratio of the mixtures was 0.943. The mixture with 25% micron has a slightly larger pressure exponent than the mixture with 50% micron aluminum (0.65 versus 0.57). Both mixtures had a slightly larger pressure exponent than the pure 80-nm ALICE mixture (0.405). The larger pressure exponents of mixtures with micron aluminum may result from lower combustion efficiency of these mixtures at low pressures. Consistent with previous observations on the pressure dependence of aluminum and ice mixtures (Risha et al., 2009, 2013), the present results suggest that combustion of bimodal mixtures will benefit from high-pressure operation.

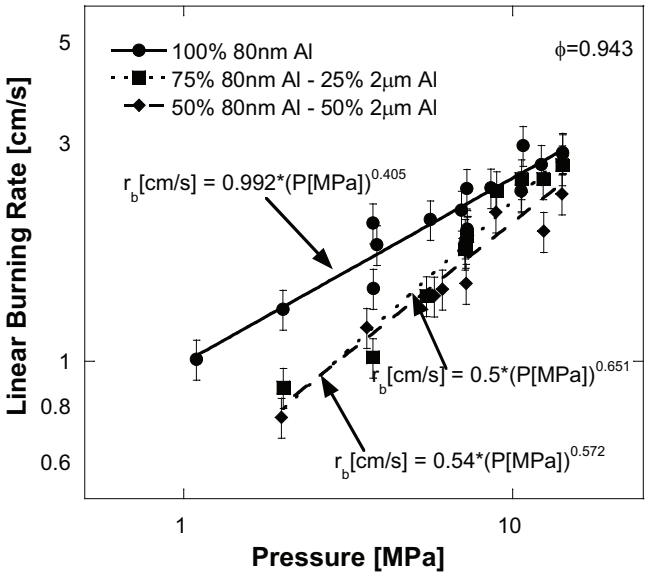

FIG. 8: Linear burning rates as a function of pressure for mixtures with 100% 80-nm aluminum and mixtures with 25% and 50% (by active weight) 2-μm aluminum. All mixtures had an equivalence ratio of 0.943.

3.2 Thrust and Isp Measurements

A comparison of motor experiments with propellant grains of equivalence ratios 0.71 and 0.943 for 100% 80-nm aluminum mixtures is presented in Figs. 9 and 10. The times were shifted so the peak pressures and peak thrusts are aligned. Figure 9 presents the chamber pressure and Fig. 10 presents the motor thrust. Even though the grain with an equivalence

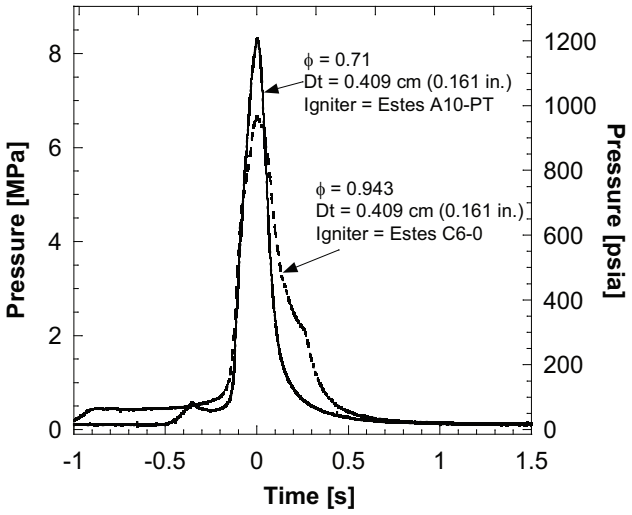

FIG. 9: Comparison of chamber pressure in the 1.91-cm center-perforated grain motor for equivalence ratios of 0.71 and 0.943; the aluminum particle diameter is 80 nm.

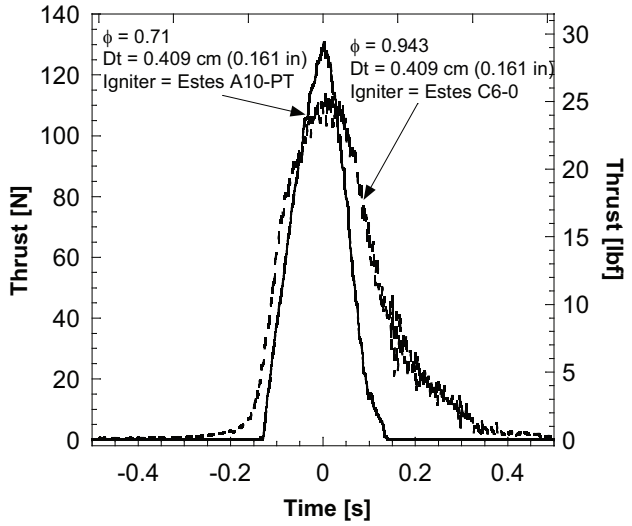

FIG. 10: Comparison of thrust from the 1.91-cm center-perforated grain motor for equivalence ratios of 0.71 and 0.943; the aluminum particle diameter is 80 nm.

ratio of 0.943 had a slightly larger igniter, ignition delays of the near-stoichiometric mixture were longer than those of the fuel-lean mixture with an equivalence ratio of 0.71. The combustion duration is also slightly longer for the mixture with $\phi = 0.943$, which is consistent with the slightly lower linear burning rates of the $\phi = 0.943$ mixtures compared to those of the $\phi = 0.71$ mixtures (Risha et al., 2009, 2013). The peak pressure and peak thrust are lower for the $\phi = 0.943$ mixture.

Figure 11 reports the chamber pressure measurements from three motor experiments with ALICE grains with no micron aluminum and 25% and 50% 2-μm aluminum, all with equivalence ratios of 0.943 and an Estes C6-0 igniter motor. The times were again shifted so that the peak pressures are nearly aligned. As can be seen from the data, the peak pressures decrease and the burning time duration increases with substitution of μAl for nAl. The corresponding thrust measurements are shown in Fig. 12 indicating a similar trend as the pressure measurements, i.e., with the addition of micron aluminum, the peak thrust decreases and the burning duration increases. These trends are consistent with the slower linear burning rates of formulations with micron aluminum.

Table 1 shows a summary of the performance characteristics of the ALICE motors with varied equivalence ratio and bimodal fuel particles. For the mixtures with $\phi = 0.943$, the active aluminum content increased from 74.5% to 84.8% as the mixture composition changed from 100% nAl to a mixture with 50% nAl and 50% μAl (based upon the active aluminum mass). The characteristic velocity is observed to increase with micron particle addition, while the C^* efficiency initially changes much more slowly and then increases

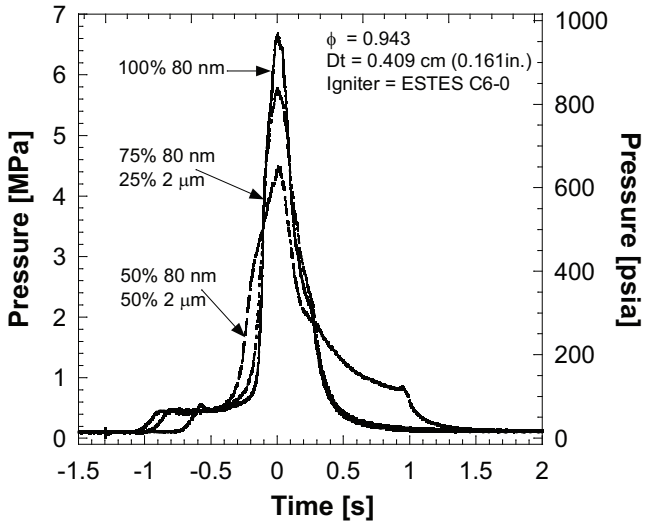

FIG. 11: Pressure measurements from the 1.91-cm diameter center-perforated grain motor with nozzle diameter of 0.161 in. and equivalence ratio of 0.943 for grains with the fuel consisting of no micron aluminum and 25% and 50% (by active mass) 2-μm aluminum.

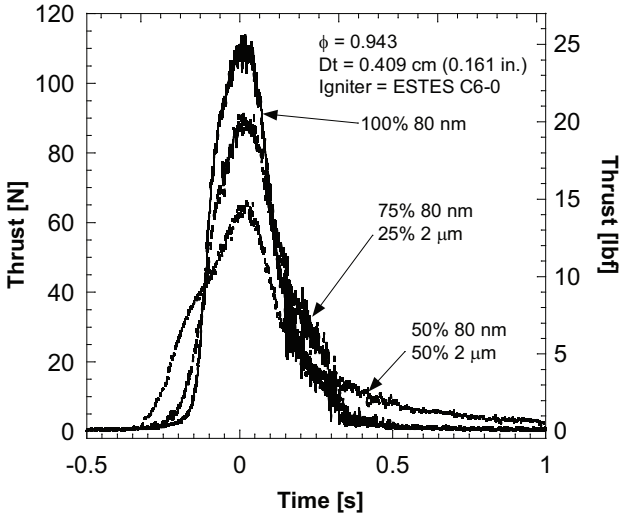

FIG. 12: Thrust measurements from the 1.91-cm-diameter center-perforated grain motor with nozzle diameter of 0.161 in. and equivalence ratio of 0.943 for grains with the fuel consisting of no micron aluminum and 25% and 50% (by active mass) 2-μm aluminum.

TABLE 1: Performance characteristics of 0.75-in. center-perforated grain motor

Parameter	**Results**			
Equivalence ratio	0.71	0.943	0.943	0.943
80-nm Novacentrix Al (%)	100	100	75	50
2-μm Valimet Al (%)	0	0	25	50
Active Al content (%)	74.5	74.5	79.6	84.8
Peak thrust (N)	133	115	91	66
C^*,avg (m/s)	582	670	675	881
$\eta_{C^*,\mathrm{avg}}$ (%)	48	56	55	70
I_{tot} (N·s)	17.5	29	26	26
Isp (s)	63	96	90	89
$\eta_{Isp,\mathrm{avg}}$ (%)	27	43	39	38
Mass remaining (%)	20.7	34.5	36.2	42
$\eta_{Isp,\mathrm{avg}}$ (%) AP/HTPB (Isp, theor = 240 s)	57			
$\eta_{C^*,\mathrm{avg}}$ (%) AP/HTPB (C^*_{theor} = 1466 m/s)	87			

Note: C^*,avg is calculated using the average nozzle throat diameter.

by ∼25% with the addition of 50% micron aluminum. Also evident from the table, Isp and Isp efficiency are nearly independent of the replacement of nAl with μAl (∼8% decrease is observed in going from 100% nAl to the 50% nAl/50% μAl mixture). As

one would anticipate a slight increase in Isp with the substitution of micron aluminum for nanometer aluminum, these results suggest larger alumina particles in the exhaust may cause two-phase losses, thereby reducing Isp while still increasing combustion efficiency. Visually this has been evident from the motor exhaust plumes, which are much brighter and often contain particle streaks compared to the plumes from grains without any micron particles. Even so, the performance is not hindered by the presence of the micron aluminum. To enhance the micron particles burning within the chamber, longer post-combustion chambers can be employed, thereby increasing the residence time of the rocket engine providing more time for the micron particles to react. These studies are currently underway. The percent mass remaining in the motor was observed to increase for the 100% nm aluminum with increasing equivalence ratio and for the ϕ = 0.943 mixtures with increasing micron aluminum content. Equilibrium analysis (McBride and Gordon, 1996) of the combustion temperatures and product composition indicate that the higher temperatures of the mixtures with ϕ = 0.943 significantly reduce the amount of solid-phase aluminum oxide in the combustion chamber (Table 2). The mixtures with an equivalence ratio of 0.71 have combustion temperatures constrained by the melting temperature of alumina due to the increasing mass fraction of the diluent water contained in the reactant mixture. However, performance slightly increases because the additional water drives the product molecular weight down, as evident from the decrease in the product Al_2O_3 mole fraction. For the ϕ = 0.943 composition, the molten alumina is solidified at the exit of the nozzle. Table 2 also indicates that the calculated exit pressure for the ϕ = 0.943 mixture is higher than the case of ϕ = 0.71.

In addition, AP/HTPB composite results are included in Table 1, which also yield low C^* and Isp efficiencies since the motor used to conduct these experiments was a

TABLE 2: Equilibrium analysis of ALICE with equivalence ratios of 0.71 and 0.943

	$\boldsymbol{\phi = 0.71}$			$\boldsymbol{\phi = 0.943}$		
	Chamber	Throat	Exit	Chamber	Throat	Exit
Pressure (bar)	68.9	41.8	1.15	68.9	40.4	1.39
Temperature (K)	2327	2327	1769	2746	2628	2327
Isp (s)			208			202
C^* (m/s)			1224			1198
Composition						
H	0.00088	0.00113	0.00017	0.00573	0.00477	0.00665
H_2	0.55414	0.55394	0.55467	0.68069	0.68170	0.68026
H_2O	0.22651	0.22647	0.22670	0.04388	0.04384	0.04373
OH	0.00007	0.00009	0.00000	0.00011	0.00008	0.00008
$Al(OH)_3$	0.00004	0.00003	0.00017	0.00001	0.00001	0.00000
Al_2O_3(l)	0.19943	0.13099	0.00000	0.26911	0.26935	0.01847
Al_2O_3(a)	0.01893	0.08734	0.21846	0.00000	0.00000	0.25069

small lab-scale system and therefore losses due to heating the chamber would be more significant than in a larger system. Since thermal losses affect chemical conversion of the reactants, the overall conversion efficiency decrease would be reflected in the C^* and Isp efficiencies.

4. CONCLUSIONS

A bimodal Al particle distribution consisting of nanometer and micron particles was studied in the reaction of aluminum with ice. Addition of micron aluminum to a nanometer-based propellant indicated a slight increase in burning rate and then a decrease in burning rate as the fraction of micron aluminum in the particle mixture was increased. Motor performance was not hindered by the presence of the micron aluminum. Mixtures with equivalence ratios closer to stoichiometric than fuel lean indicated substantial improvements in the C^* and Isp efficiencies. The higher temperatures of the near stoichiometric mixtures enable the formation of molten alumina thus improving the reactivity of the nanometer and micron aluminum. Future studies will continue to examine the combustion characteristics of bimodal distributions of aluminum particles in larger-size motors and over a wider range of mixture ratios.

ACKNOWLEDGMENTS

The authors would like to thank AFOSR and NASA for funding this program under Contract No. FA9550-07-1-0582. Special thanks go to Mr. Rob Uhlig, Mr. Bryan Sones, and Mr. Lynn Witherite of the Pennsylvania State University Applied Research Laboratory (ARL) for their assistance and to ARL for usage of the Steam Plant test cell facilities in conducting the motor firings. The authors thank Mr. Ed Roemer of LANL and Dr. Justin Sabourin of Penn State for the SEM micrographs of the particles.

REFERENCES

Connell, Jr., T. L., *Combustion of Aluminum and Ice Based Solid Propellants for Propulsion Applications and High Temperature Hydrogen Generation*, Master's Thesis, The Pennsylvania State University, 2011.

Franson, C., Orlandi, O., Perut, C., Fouin, G., Chauveau, C., Gokalp, I., and Calabro, M., Al/H_2O and Al/H_2O/H_2O_2 frozen mixtures as examples of new composite propellants for space applications, In *Proc. of 7th International Symposium on Launcher Technologies*, organized by CNES, April 2–5, Barcelona, Spain, 2007a.

Franson, C., Orlandi, O., Perut, C., Fouin, G., Chauveau, C., Gokalp, I., and Calabro, M., New high energetic composite propellants for space applications: Refrigerated solid propellant (RSP), In *Proc. of 2nd European Conference for Aerospace Sciences (EUCASS)*, Brussels, Belgium, 1–6 July, 2007b.

Ingenito, A. and Bruno, C., Using aluminum for space propulsion, *J. Propul. Power*, vol. **20**, no. 6, pp. 1056–1063, 2004.

Ivanov, V., Ivanov, V. G., Gavriluk, O. V., and Glazkov, O. V., Combustion of electroexploded aluminum in liquid media, *Proc. JANNAF Propulsion Meeting*, Tampa, FL, 1995.

Ivanov, V. G., Gavrilyuk, O. V., Glazkov, O. V., and Safronov, M. N., Specific features of the reaction between ultra fine aluminum and water in a combustion regime, *Combust., Explos. Shock Waves*, vol. **36**, no. 2, pp. 213–219, 2000.

McBride, B. J. and Gordon, S., Computer program for calculation of complex chemical equilibrium compositions and applications, NASA, 1996.

Miller, T. F. and Herr, J. D., Green Rocket propulsion by reaction of Al and Mg powders and water, AIAA Paper 2004-4037, 2004.

Pourpoint, T. L., Wood, T. D., Pfeil, M. A., Tsohas, J., and Son, S. F., Feasibility study and demonstration of an aluminum and ice solid propellant, *Int. J. Aerospace Eng.*, vol. **2012**, pp. 874076-1–874076-11, 2012.

Risha, G. A., Huang, Y., Yetter, R. A., Yang, V., Son, S. F., and Tappan, B. C., Combustion of aluminum particles with steam and liquid water, AIAA Paper 2006-1154, 2006.

Risha, G. A., Son, S. F., Yetter, R. A., Yang, V., and Tappan, B. C., Combustion of nano-aluminum and liquid water, *Proc. Combust. Inst.*, vol. **31**, pp. 2029–2036, 2007.

Risha, G. A., Sabourin, J. L., Yang, V., Yetter, R. A., Son, S. F., and Tappan, B. C., Combustion and conversion efficiency of nanoaluminum-water mixtures, *Combust. Sci. Technol.*, vol. **180**, no. 12, pp. 2127–2142, 2008.

Risha, G. A., Connell, T. L., Yetter, R. A., Yang, V., Wood, T. D., Pfeil, M. A., Pourpoint, T. L., and Son, S. F., Aluminum-ice (ALICE) propellants for hydrogen generation and propulsion, AIAA Paper 2009-4877, 2009.

Risha, G. A., Connell, T. L., Sundaram, D. S., Yetter, R. A., and Yang, V., Combustion of frozen nanoaluminum and water mixtures, *J. Propuls. Power*, (submitted), 2013.

Yetter, R. A., Risha, G. A., and Son, S. F., Metal particle combustion and nanotechnology, *Proc. Combust. Inst.*, vol. **32**, pp. 1819–1838, 2009.